Int. J. Cancer: **117,** 923–933 (2005)
© 2005 Wiley-Liss, Inc.

PPARγ-dependent effects of conjugated linoleic acid on the human glioblastoma cell line (ADF)

AnnaMaria Cimini[1]*, Loredana Cristiano[1], Sabrina Colafarina[1], Elisabetta Benedetti[1], Silvia Di Loreto[2], Claudio Festuccia[3], Fernanda Amicarelli[1], Rosa Angela Canuto[4] and Maria Paola Cerù[1]

[1]*Department of Basic and Applied Biology, University of L'Aquila, L'Aquila, Italy*
[2]*Institute of Transplant of Organs and Immunocytology, National Research Center, L'Aquila, Italy*
[3]*Department of Experimental Medicine, University of L'Aquila, L'Aquila, Italy*
[4]*Department of Experimental Medicine and Oncology, University of Torino, Torino, Italy*

Conjugated linoleic acid (CLA) has been shown to exert beneficial effects against carcinogenesis, atherosclerosis and diabetes. It has been demonstrated that CLA modulates lipid metabolism through the activation of peroxisome proliferator-activated receptors (PPARs). The PPAR family comprises 3 closely related gene products, PPAR α, β/δ and γ, differing for tissue distribution, developmental expression and ligand specificity. It has also been demonstrated that activated PPARγ results in growth inhibition and differentiation of transformed cells. These observations stimulated a great interest toward PPARγ ligands as potential anticancer drugs to be used in a differentiation therapy. Glioblastomas are the most commonly diagnosed primary tumors of the brain in humans. The prognosis of patients with high-grade gliomas is poor and only marginally improved by chemotherapy. The aim of this work was to study the effects of CLA and of a specific synthetic PPARγ ligand on cell growth, differentiation and death of a human glioblastoma cell line as well as on parameters responsible for the metastatic behavior of this tumor. We demonstrate here that CLA and PPARγ agonist strongly inhibit cell growth and proliferation rate and induce apoptosis. Moreover, both treatments decrease cell migration and invasiveness. The results obtained show that CLA acts, directly or indirectly, as a PPARγ activator, strongly suggesting that this naturally occurring fatty acid may be used as brain antitumor drug and as a chemopreventive agent. Moreover, the γ-agonist, once experimented and validated on man, may represent a useful coadjuvant in glioblastoma therapy and in the prevention of recurrences.
© *2005 Wiley-Liss, Inc.*

Key words: peroxisome proliferator-activated receptors; fatty acids; tumor cells; apoptosis; cell proliferation

Several studies have provided convincing evidence that dietary fats play important but different roles in tumorigenesis.[1,2] Saturated fatty acids (FAs) and n-6 polyunsaturated FAs (PUFAs) have growth-promoting effects on many tumors,[3] while n-3 PUFAs apparently inhibit tumorigenesis.[4] Moreover, effects of PUFAs are different in relation to the cell type and differentiation degree and to the normal or malignant status of the cells.[5–8] Conjugated linoleic acid (CLA), a positional and geometric isomer of linoleic acid, has been shown to exert beneficial effects against carcinogenesis, atherosclerosis and diabetes, to enhance immunologic function while protecting against the catabolic effects of immunostimulation and to affect tissue body composition.[9–11] It has been recently demonstrated that CLA modulates lipid metabolism through the activation of peroxisome proliferator-activated receptors (PPARs).[12–14]

PPARs belong to the steroid/thyroid/retinoid and vitamin D3 receptor superfamily and play fundamental roles in energy homeostasis by mediating FA action on the expression of genes involved in lipid metabolism.[15,16] As other ligand-activated transcriptional factors of this superfamily, PPARs heterodimerize with 9-cis retinoic acid receptors (RXRs) and interact with specific DNA response elements (PPRE) located upstream to the target genes. These include genes not only involved in lipid metabolism,[17] but also regulating cell cycle and differentiation.[18] The PPAR family comprises 3 closely related gene products, PPARα, β/δ and γ,[19,20] differing for tissue distribution, developmental expression and ligand specificity.[16]

Whereas PPARα operates in the catabolism of FAs and eicosanoids and the precise functions of the β/δ isotype are yet to be clarified, PPARγ regulates genes implicated in lipogenic pathways and is involved in adipocyte differentiation.[21] Recently, it has also been demonstrated that PPARγ plays important roles in inflammation and regulation of cell proliferation, differentiation and death.[18] As regards PPARγ ligands, 15-deoxy-Δ12,14 prostaglandin J2 (PGJ2) is the most potent natural ligand,[22,23] while the antidiabetic drugs thiazolidinediones (TZD) have been recognized as effective synthetic PPARγ agonists.[24] Ligand-activated PPARγ results in growth inhibition and differentiation of normal and transformed cells.[25,26] These observations stimulated great interest in PPARγ ligands as potential anticancer drugs to be used in a differentiation therapy.[27,28] Although data on this topic are somewhat controversial, probably depending on the specific tumor and on the *in vivo* or *in vitro* models, extending these studies to other tumor cell types and possibly to other PPARγ ligands appears very promising.

Glioblastomas are the most commonly diagnosed primary tumors of the brain in humans.[29] These highly aggressive tumors are characterized by rapid proliferative rate and invasiveness as well as by the secretion of angiogenetic factors and proteins leading to T-cell immunosuppression.[30] The prognosis of patients with high-grade gliomas is poor and only marginally improved by chemotherapy.[31]

PPARs have been demonstrated to be expressed by glioblastoma and astrocytoma[8,32,33] cell lines, although to levels that differ from their normal counterpart.[34] The aim of this work was to study the effects of CLA and of a specific synthetic PPARγ ligand[35] on cell growth, differentiation and death of a human glioblastoma cell line as well as on parameters responsible for the metastatic behavior of this tumor.

Material and methods

Reagents

CLA was generously provided by Natural Lipids (Hovdebygda, Norway); Triton X-100, Nonidet P40, sodium dodecylsulfate, Tween 20, L-glutamine, phalloidin-TRITC, anti-GFAP monoclonal antibody, FITC-labeled antirabbit and antimouse IgG antibodies and PVDF were purchased from Sigma Chemical (St. Louis, MO); ELISA nucleosome detection kit, BrdU incorporation kit and RNAase were from Roche Diagnostic (Indianapolis, IN); trypsin-EDTA solution, streptomycine-penicillin, TRIzol reagent and Platinum Taq RNA plymerase were from Gibco Invitrogen (San Giuliano Milanese [MI], Italy); anti-PPARγ antibodies were from Affinity Bioreagents (Golden, CO) for the immunofluorescence

Grant sponsor: Banco San Paolo, Torino; Grant sponsor: Italian PRIN 2003; Grant sponsor: Neuromed 1% Sanità 2003.
***Correspondence to:** Department of Basic and Applied Biology, University of L'Aquila, Via Vetoio n. 10, 67010 Coppito, AQ, Italy. Fax: +39-0862-433273. E-mail: cimini@univaq.it
Received 25 January 2005; Accepted after revision 18 April 2005
DOI 10.1002/ijc.21272
Published online 28 June 2005 in Wiley InterScience (www.interscience.wiley.com).

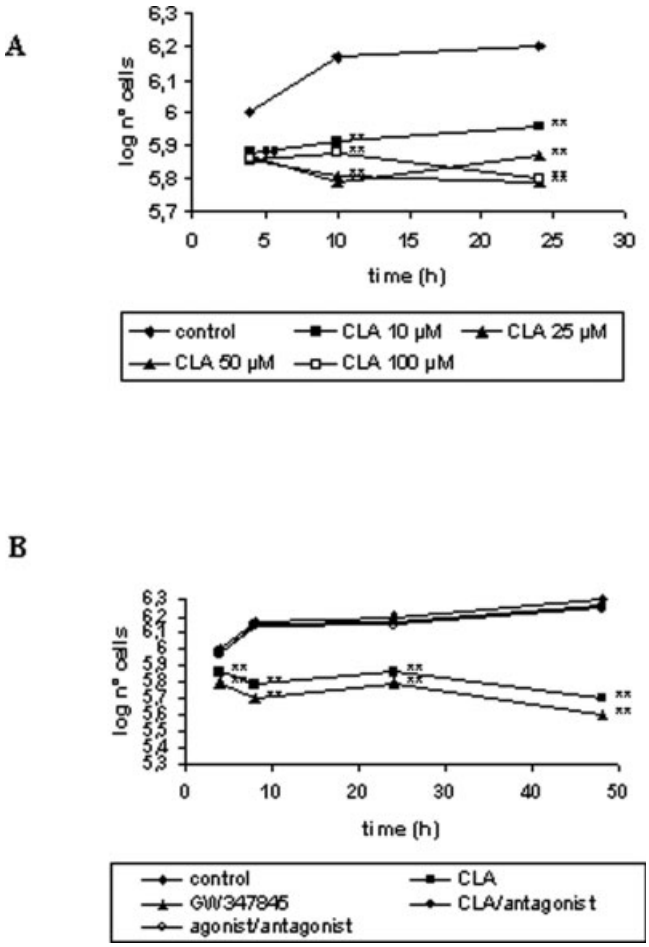

Figure 1 – Semilog growth curves of control and treated ADF cells. After treatments, Trypan blue-excluding cells were counted at different time points. (*a*) Effect of different concentrations of CLA at various time points (4, 8 and 24 hr). (*b*) Effects of 25 μM CLA and of 1 μM PPARγ agonist GW347845X, both alone or in combination with the PPARγ antagonist GW259662 (1 μM), used for different time points (4–48 hr). Data are mean ± SD of 6 different experiments run in triplicate. SD never exceeded 10%. Asterisk, $p < 0.01$; double asterisk, $p < 0.001$.

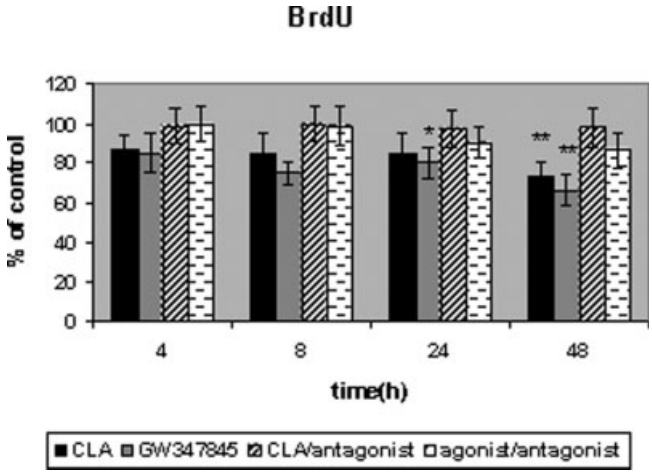

Figure 2 – BrdU incorporation expressed as percentage of the control values in cells treated with 25 μM CLA or 1 μM GW347845X and combination of both with 1 μM GW259662 for different time points (4–48 hr). Data are mean ± SD of 6 different experiments run in triplicate. SD never exceeded 10%. Asterisk, $p < 0.01$; double asterisk, $p < 0.001$.

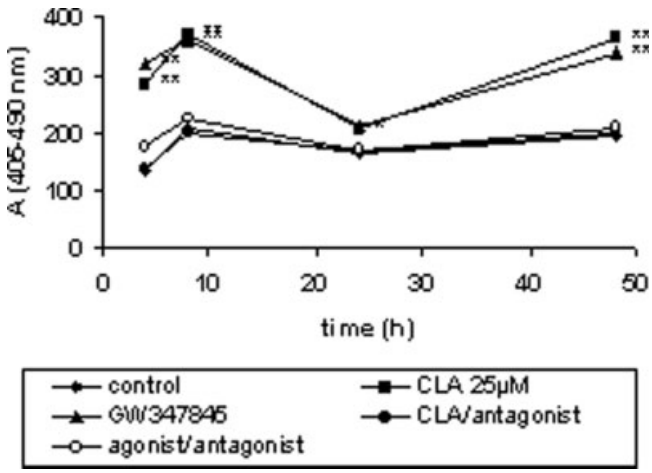

Figure 3 – Apoptotic rate in control and treated cells. Apoptosis was evaluated as nucleosome concentration; 25 μM CLA and 1 μM GW347845X significantly induced apoptotic events and the effect was reverted by 1 μM GW259662. Data are mean ± SD of 4 experiments run in triplicate, with SD never exceeding 10%. Asterisk, $p < 0.01$; double asterisk, $p < 0.001$.

experiments, while for immunoblotting anti-PPARγ and rabbit anti-Erk1,2, anti-P-Erk, anticaspase-3, anticaspase-9 were from Santa Cruz Biotechnology (Santa Cruz, CA); RPMI-1640 and fetal bovine serum (FBS) were from Euroclone (Wetherby, West Yorkshire, UK); Vectashield was from Vector (Burlingame, CA); ECL kit was from Amersham Life Sciences (Buckinghamshire, U.K.); micro-BCA protein detection kit was from Pierce (Rockford, IL); Gene Specific Realtime RT-PCR kit was from Ambion (Austin, TX); Transam PPARγ kit was from Activemotif (Carlsbad, CA). All other chemicals were of the highest analytical grade. The PPARγ agonist and antagonist, GW347845X and GW259662, respectively, were generous gifts of Dr. Timothy M. Willson, GlaxoSmithKline (Research Triangle Park, NC).

Cell cultures

Human glioma cell line (ADF) was a generous gift of Professor P.G. Natali (Istituto Regina Elena, Rome, Italy). Cells were seeded at 3×10^4 cells/cm^2 and maintained in monolayer culture in RPMI-1640 medium supplemented with 10% FBS for 24 hr before treatments. For treatments with CLA and PPARγ ligand and antagonist, FBS was replaced with charcoal (5 mg/ml)-stripped serum (overnight at 4°C) in order to eliminate endogeneous lipid components.

Treatments

CLA was prepared from a solution containing 1 mM CLA, 1 mM NaOH, 10 mg/ml defatted BSA in serum-free medium. The solution was incubated for 10 min at 37°C and sonicated (5 cycles of 5 sec), incubated at 50°C for 10 min and used at the indicated concentrations. The PPARγ ligand, GW347845X, was dissolved in 0.01% DMSO and used at the final concentration of 1 μM. The PPARγ antagonist GW259662 was used at 1 μM (final concentration) and administered 30 min before CLA or GW347845X treatment. Controls received the vehicle alone (0.001% DMSO for GW347845X and GW259662, delipidated serum for CLA).

Cell growth, proliferation and death assays

Cell growth curves were obtained by counting Trypan blue-excluding cells, both in control and in treated cultures, at different time points. Cell proliferation was measured by BrdU incorporation assay according the manufacturer's directions.

For apoptosis detection, cells were seeded in 96-well plates at a density of 3×10^4 cells/cm^2 in delipidated serum. Control and treated cells were analyzed for apoptosis using an ELISA nucleosome detection kit. Absorbances at 405 and 490 nm were recorded according the manufacturer's directions.

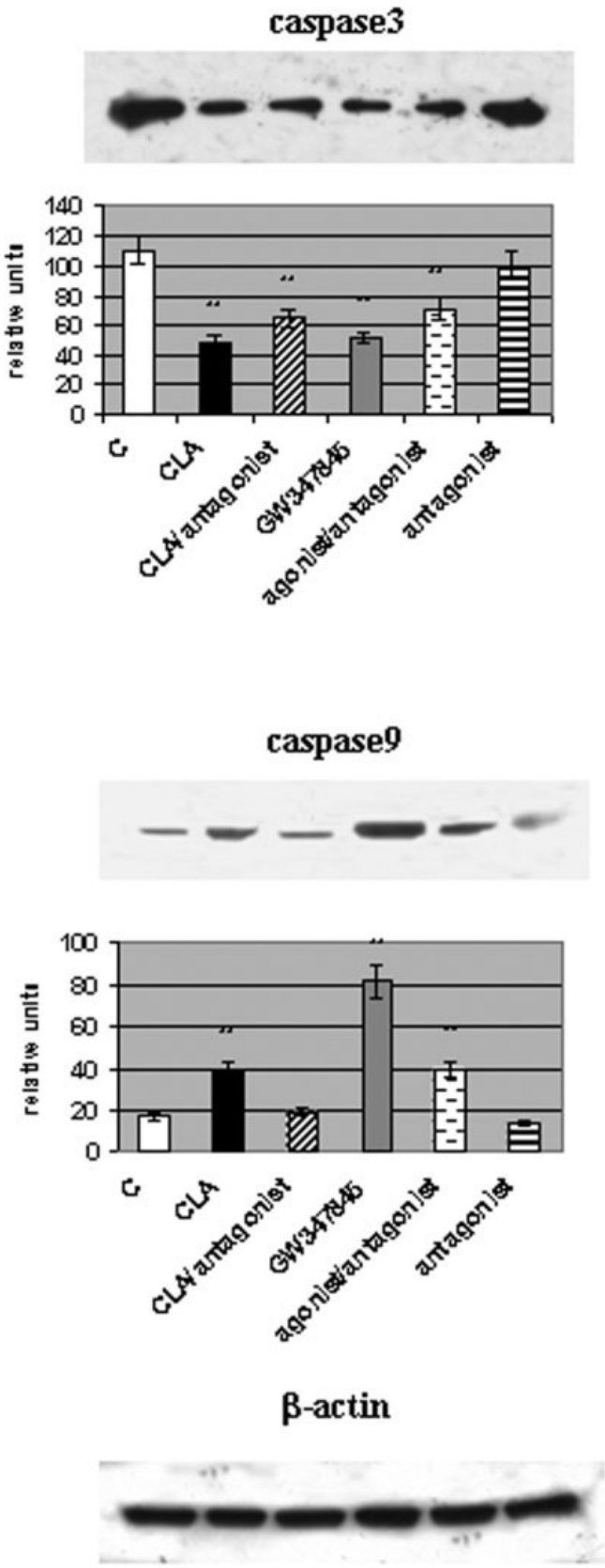

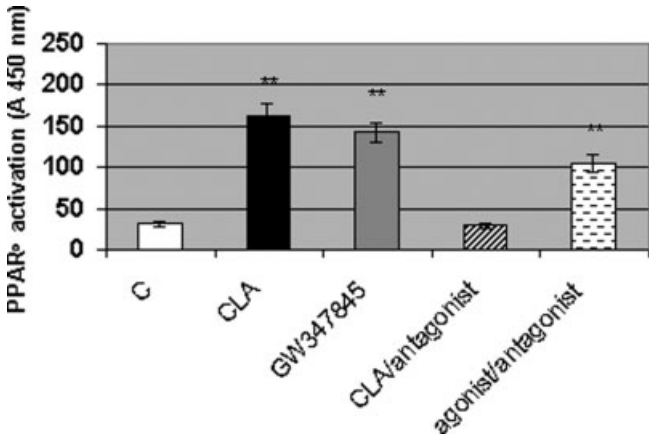

FIGURE 5 – PPARγ transactivation assay in control and treated cells. Treatments as in Figure 4. Data are mean ± SD of 3 experiments run in quadruplicate. Asterisk, $p < 0.01$; Double asterisk, $p < 0.001$.

Protein assay

Proteins were assayed by the micro-BCA kit.

PPARγ transactivation assay

PPARγ transactivation was checked by Transam PPARγ kit (Activemotif) according the manufacturer's directions. The Transam kits is a highly sensitive ELISA-based assays that facilitate the study of transcription factor activation in mammalian tissue and cell extracts. Each transam kit contains a 92-well plate, to which oligonucleotide containing a consensus-binding site has been immobilized. The transcription factor of interest binds specifically to the oligonucleotide. The revelation is done by the incubation with a primary antibody specific for the active form of bound transcription factor, followed by the incubation with an HRP-conjugated secondary antibody. After the incubation with standard developing solution, the samples are quantified by an ELISA plate reader (450 nm). Positive and negative controls are run in parallel.

Immunoblotting

For Western blotting, cells treated for 4 hr were washed in ice-cold PBS and harvested in ice-cold RIPA buffer (phosphate buffer saline, pH 7.4, containing 0.5% sodium deoxycolate, 1% Nonidet P-40, 0.1% sodium dodecyl sulfate, 5 mM EDTA, 100 mM sodium fluoride, 2 mM sodium pirophosphate, 1 mM PMSF, 2 mM ortovanadate, 10 μg/ml leupeptin, 10 μg/ml aprotinin, 10 μg/ml pepstatin). Cell lysates were centrifuged and the supernatants were assayed for protein content; 40 μg of proteins from whole cell lysates were electrophoresed through a 10% SDS-polyacrilamide gel under reducing conditions.[36] Proteins were transferred onto PVDF membrane sheets and nonspecific binding sites were blocked by overnight incubation at 4°C in 20 mM TRIS, 55 mM NaCl and 0.1% Tween 20, pH 7.4 (TST), containing 5% nonfat dry milk (blocking solution). Membranes were then incubated for 1 hr at room temperature (RT) with rabbit anti-PPARγ,

FIGURE 4 – Western blottings and relative densitometric analyses for caspase-3 (inactive form) and -9 (active form) in control and treated cells (25 μM CLA and 1 μM GW347845X, with or without 1 μM GW259662, for 4 hr). As loading control, β-actin was used. For all conditions, an example of Western blotting is shown. Densitometric data are mean ± SD of 5 experiments. Asterisk, $p < 0.01$; double asterisk, $p < 0.001$.

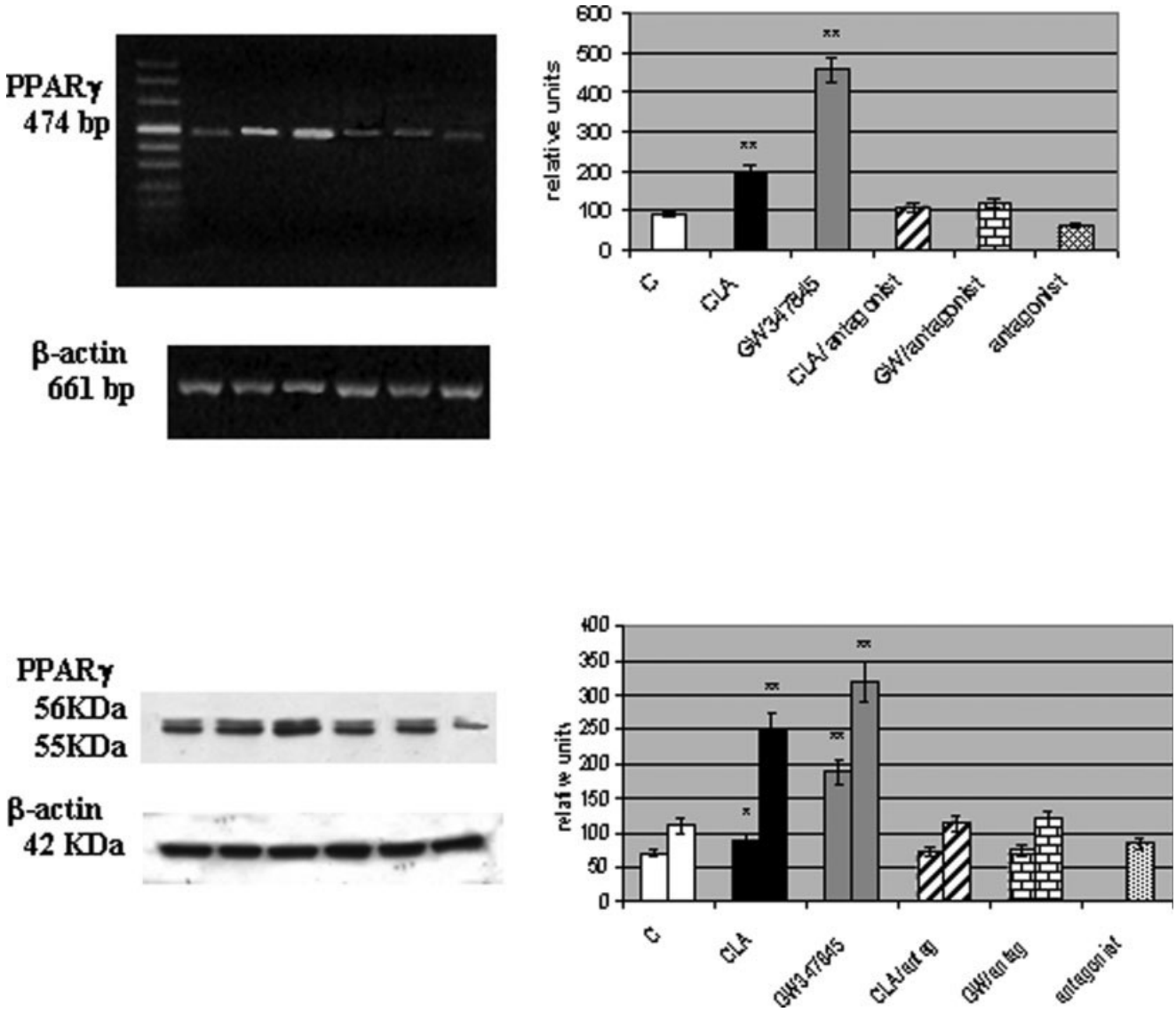

FIGURE 6 – Western blotting and RT-PCR for PPARγ and relative densitometric analyses in control and treated cells. Treatments as in Figures 4 and 5. The densitometric values are mean ± SD of 3 experiments. For the immunoblottings, both the PPARγ1 and PPARγ2 bands (lighter and heavier, respectively) were considered. Data were normalized against β-actin. Asterisk, $p < 0.01$; double asterisk, $p < 0.001$.

anti-ERK, or anti-P-ERK antibodies (1:1,000) or with anticaspase-3 or -9 (1:200) dissolved in the blocking solution. After extensive washings with TST, the membranes were incubated with HRP-conjugated antirabbit IgG secondary antibody (1:2,000). Immunoreactive bands were visualized by chemiluminescence (ECL).

RT-PCR analysis

Total cellular RNA was extracted by TRIzol reagent according to the manufacturer's directions. The total RNA concentration was determined spectrophotometrically in RNAase-free water. Reverse transcription (RT) was performed using Gene Specific Realtime TR-PCR kit and polymerase chain reaction (PCR) amplification of specific target RNA was performed using Platinum Taq DNA polymerase following the manufacturer's directions. The following primers were used. Human PPARγ: 5′-TCTCTCCGTAATGGAAGACC-3′ (upstream) and 5′-GCATTATGAGACATCCCCAC-3′ (downstream). Amplification conditions were 30 sec at 94°C (denaturation), 1 min at 66°C (annealing), 1 min at 72°C (extension) for 40 cycles. The amplification product was 474 bp. Human β-actin: 5′-TGACGGGGTCACCCACACTGTGCCCATCTA-3′ (upstream) and 5′-CTAGAAGCATTGCGGTGGACGATGGAGGG-3′ (downstream). Amplification conditions were: 40 sec at 94°C (denaturation), 40 sec at 65°C (annealing), 1 min at 72°C (extension). The amplification product was 661 bp. PCR products were electrophoretically separated on 1.5% agarose gel and identified by ethidium bromide staining. To normalize differences in total RNA concentration among samples, bands were normalized against β-actin. Semiquantitative analysis was performed by Total Lab V.I.II. System (Phoretics, New Castle, UK).

Morphology

For purely morphologic observation, cells were seeded on coverslips (3×10^4 cells/cm^2), treated for 48 hr and fixed for 10 min at RT in 4% paraformaldehyde in PBS and analyzed by phase contrast microscopy.

Immunofluorescence

Cells grown on coverslips (3×10^4 cells/cm^2) and treated for 48 hr were fixed for 10 min at RT in 4% paraformaldehyde in PBS

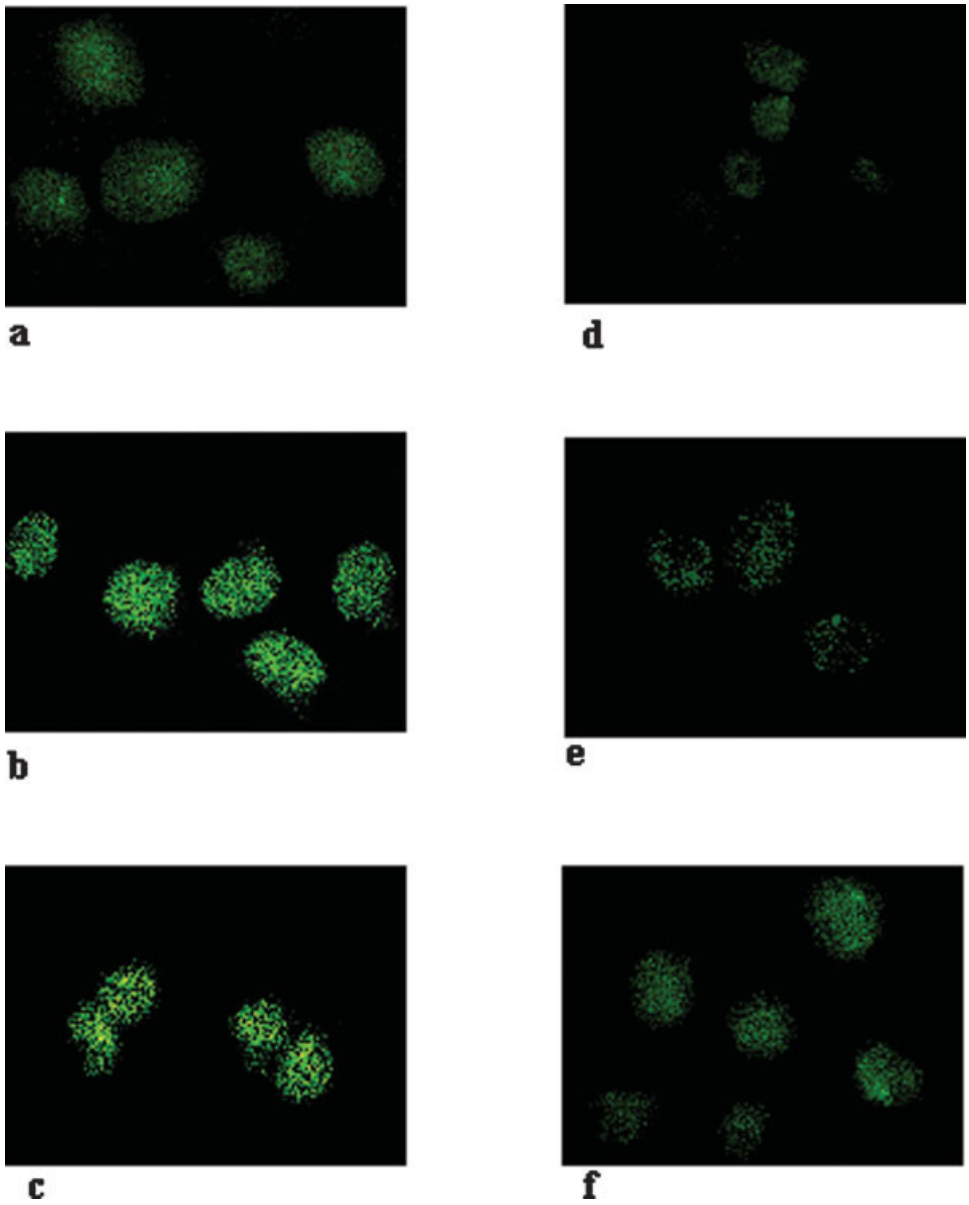

FIGURE 7 – PPARγ immunolocalization in control and treated cells. Treatments were for 4 hr: (*a*) control; (*b*) 25 μM CLA; (*c*) 1 μM GW347845X; (*d*) 1 μM GW259662; (*e*) CLA/antagonist; (*f*) agonist/antagonist. PPARγ was always localized to the nucleus; CLA and GW347845X increased the fluorescence intensity and GW259662 reverted this effect. Magnification: 300×.

and permeabilized in PBS containing 0.1% Triton X-100 for 10 min at RT. Cells were then incubated with anti-PPARγ or N-cadherin (1:100 or 1:1,000 in PBS containing 3% BSA, respectively) antibodies overnight at 4°C. After extensive washings with PBS, cells were incubated with fluorescein-labeled antirabbit IgG secondary antibodies (1:100 in PBS containing 3% BSA) for 30 min at RT. Actin staining was performed incubating fixed cells with phalloidin-TRITC (1:100 in PBS containing 3% BSA) for 30 min at RT. After extensive washings with PBS, cells were mounted with Vectashield mounting medium and photographed at fluorescence microscope (Axiophot; Zeiss, Oberkochen, Germany).

Cell adhesion, migration and invasiveness assay

For adhesion, control and 48-hr-treated cells were seeded onto plastic Matrigel (25 μg/ml) or gelatin (0.1% v/v)-coated 96-well (2×10^4 cells/well) in serum-free medium and incubated at 37°C, for 15, 30 and 60 min. Cells were then washed twice with PBS and fixed with ice-cold methanol for 10 min. After washings, cells were allowed to air-dry for 5 min and stained with 20 μl/well 0.5% (w/v) crystal violet for 15 min at RT. After washings, cells were covered with methanol for 15 min until no more staining was released. Absorbance at 595 of methanol is directly proportional to adhesion grade.

Migration and invasiveness assays were performed on Boyden chambers containing PVPF8 filters coated by gelatin 0.1% (v/v) or Matrigel (25 μg/ml), respectively. Control and 48-hr-treated cells were detached, washed twice with PBS and resuspended in serum-free medium at 7×10^5 cells/ml; 600 μl of cell suspension was seeded in the upper chamber and allowed to migrate for 6 hr. After removing the nonmigrated cells on the upper face of the filter, the migrated ones on the lower face of the filter were stained with Deef-Quick, mounted on slides and counted under light microscope. For each conditions, 3 filters were prepared, and for each filter, 5 fields were counted.

Protease expression and MMP activation assay

Expression and activation of gelatinase A (pro-MMP-2) and gelatinase B (pro-MMP-9) were analyzed by zymography performed using an SDS-polyacrylamide 8.5% gel copolymerized with 0.1 mg/ml gelatin (Sigma). Routinely, conditioned media

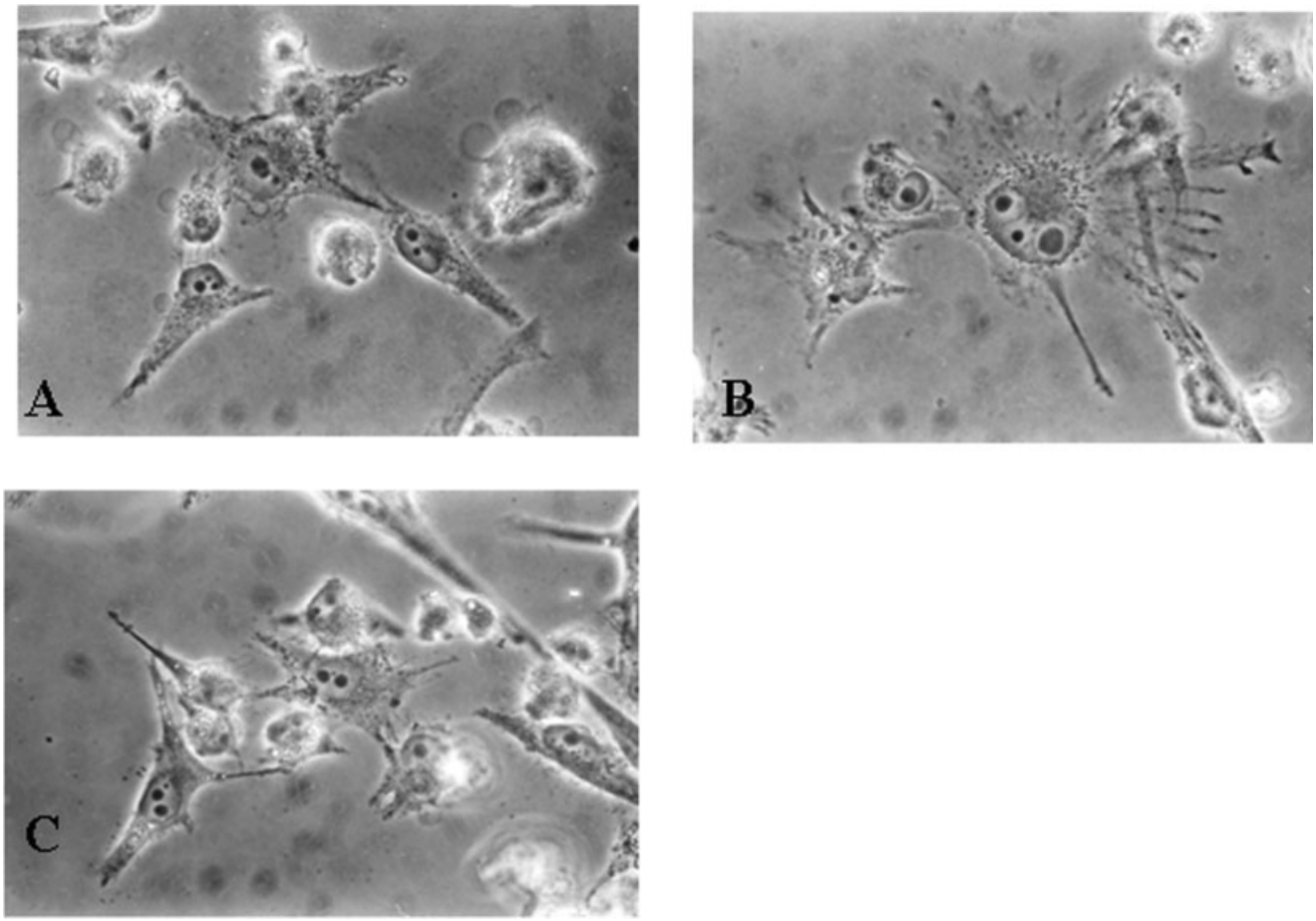

FIGURE 8 – Phase contrast microscopy of control and 48-hr-treated cells: 25 μM CLA (*b*) and, to a lesser extent, 1 μM GW347845X (*c*) affected cell morphology by inducing more evident cellular spreading and more numerous and branched cell processes than in controls (*a*). Magnification: 450×.

were obtained from cultures grown in 75 cm^2 flasks. Afterward, adhesive cells were washed with PBS and incubated 48 hr, each treated as described above. Following incubation, culture media were collected, centrifuged at top speed in an Eppendorf microcentrifuge (Eppendorf, Hamburg, Germany) for 5 min to remove cell debris and stored at −80°C until assayed. Corresponding monolayers were trypsinized and the cells counted to normalize the gelatinase activity of the conditioned media. Media were defrosted and precipitated in EtOH (1:6), then suspended in sample buffer (the corresponding medium of 8×10^5 cells/100 μl); 40 μl (corresponding to 3×10^5 cells) for lane were subjected to zymography. Gels were washed twice in H_2O containing 2.5% Triton X-100, incubated 24 hr with 50 mM TRIS-HCl, pH 7.4, containing 5 mM $CaCl_2$ and stained with Blue Coomassie for 30 min at RT. Gels were then destained with EtOH/acetic acid (30% to 7%).

Statistics

Statistical significance of paired samples was analyzed by Student's *t*-test (double asterisk, $p < 0.01$; triple asterisk, $p < 0.001$). For RT-PCR analysis, samples were processed by SPSS software and analyzed by ANOVA test, followed by Scheffe's *posthoc* test analysis (double asterisk, $p < 0.005$; triple asterisk, $p < 0.001$).

Results

In preliminary experiments, the effect of delipidated serum on cell growth rate was assessed. Since delipidated serum did not affect cell growth (not shown), we decided to use it in all subsequent experiments in order to eliminate possible interferences by lipid components normally present in the serum.

Cell proliferation and death

In a first series of experiments, we studied the effects of different CLA concentrations on cell growth rate at different time points. Figure 1(*a*) shows the semilog growth curves of control and CLA-treated cells. CLA caused a strong decrease in cell growth rate at all concentrations and time points tested. Since high concentrations (50–100 μM) of CLA also induced necrotic death, as demonstrated by Trypan blue staining and lactic dehydrogenase activity assayed in the culture medium (not shown), the 25 μM CLA concentration was used for all subsequent experiments.

In order to verify if the CLA-induced reduction of cell growth might be ascribed to PPARγ activation, the effects of CLA were compared with those of a specific PPARγ ligand, GW347845X. Moreover, a specific PPARγ antagonist, GW259662, administered in association with CLA or GW347845X was also tested.

Figure 1(*b*) shows the comparison between the effects of 25 μM CLA and the PPARγ ligand, GW347845X, used at a concentration of 1 μM, chosen on the basis of published data.[37] Similarly to CLA, GW347845X induced a reduction of cell number. Administration of the PPARγ antagonist, GW259662, in association with CLA or GW347845X completely reverted both CLA and GW347845X effects (Fig. 1*b*).

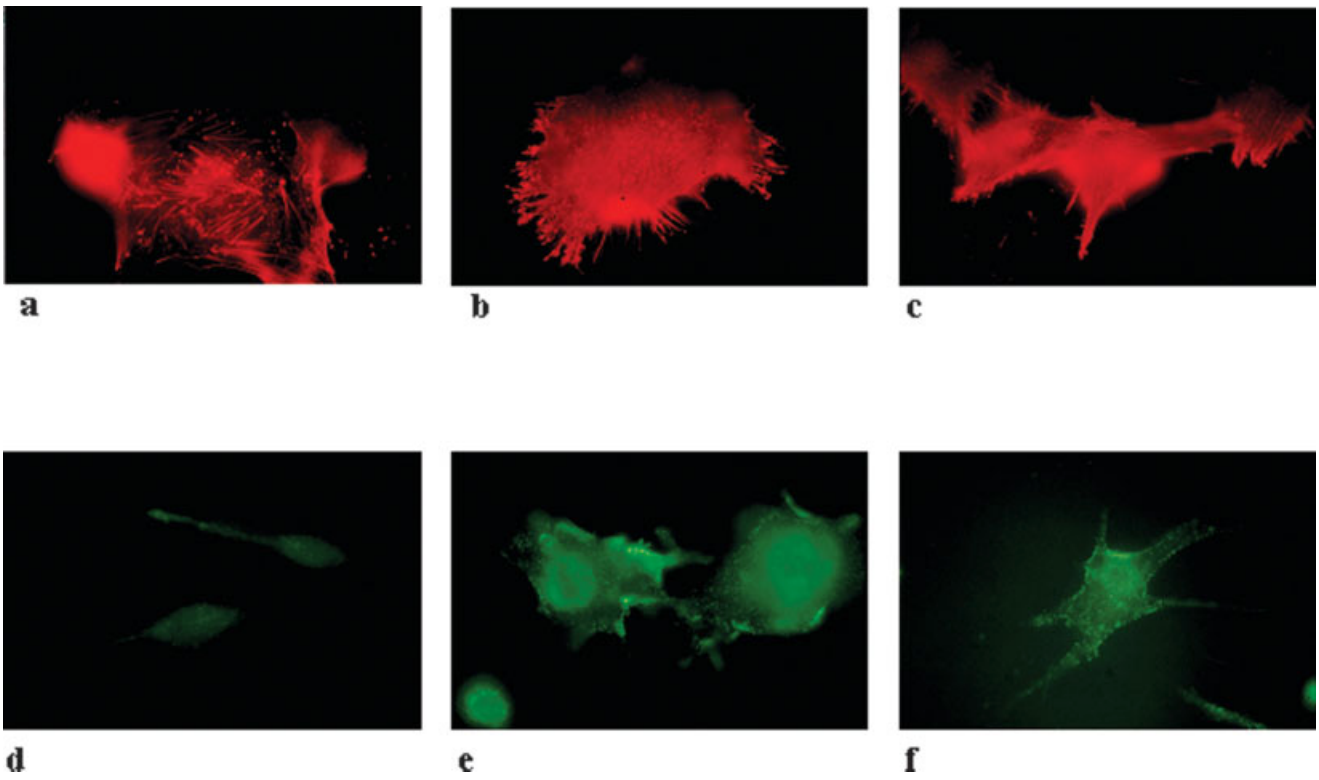

FIGURE 9 – Microfilament organization visualized by phalloidin-TRITC staining (*a*, control; *b*, 25 μM CLA; *c*, 1 μM GW347854X) and N-cadherin immunolocalization (*d*, control; *e*, CLA; *f*, GW347845X) in control and treated cells. Magnification: 330×.

Figure 2 shows the effects of the treatments on cell proliferation as evaluated by BrdU incorporation. Values are expressed as percentages of the corresponding controls. Both CLA and GW347845X treatments decreased BrdU incorporation and the effects were especially apparent after 48 hr of treatment. The antagonist completely abolished CLA or GW347845X effects at any time point tested.

Figure 3 shows the apoptotic rate, evaluated as nucleosome concentration in control and treated samples. CLA and GW347845X increased nucleosome concentration with a somewhat biphasic pattern, showing maximal activity at 8 and 48 hr. The antagonist completely abolished the CLA or GW347845X effects. The Western blotting and relative densitometric analyses of caspase-3 (inactive form) and caspase-9 (active form) are shown in Figure 4. Both CLA and PPARγ agonist reduced the level of the inactive form of caspase-3, confirming that the treatments induced apoptotic death. However, the PPARγ antagonist did not revert this effect, suggesting that activation of caspase-3 was not totally PPARγ-dependent. As regards caspase-9, both treatments induced the active form, with the agonist much more effective than CLA. Moreover, while the antagonist reverted the CLA-induced caspase-9 increase, it was not able to abolish the effect of PPARγ agonist completely, thus suggesting that some mechanism(s) other than PPARγ activation was also acting in this case.

PPARγ

The results of the PPARγ transactivation assay (Fig. 5) demonstrate that both CLA and GW347845X transactivated PPARγ. The antagonist completely reverted CLA effects, but less efficiently inhibited GW347845X effects.

In Figure 6, the Western blotting and RT-PCR analysis for PPARγ are reported. CLA and, even more dramatically, GW347845X increased PPARγ, both at protein and mRNA levels. In both cases, the association with the antagonist reverted these effects to control values.

PPARγ immunofluorescent localization in control and treated cells (Fig. 7) always shows a nuclear positivity. Both CLA and γ-agonist seemed to increase the fluorescence intensity (Fig. 7*b* and *c*), while the antagonist apparently abolished this effect.

Morphology

At the light microscopic level, untreated cells appeared as a uniform population showing a predominantly bipolar shape (Fig. 8*a*). CLA strongly modified cell morphology promoting cell spreading and processes elongation (Fig. 8*b*). The γ-agonist exerted less evident effects (Fig. 8*c*). The antagonist alone or in association had no effect on cell morphology (not shown). In Figure 9, the microfilament organization and N-cadherin localization in control and treated cells are shown. In control cells, microfilaments appeared disorganized and many focal adhesion contacts were observed (Fig. 9*a*); N-cadherin was mainly localized in the cytoplasm (Fig. 9*d*). CLA and GW347845X induced microfilament organization (Fig. 9*b* and *c*) and N-cadherin was increased and redistributed to plasma membranes (Fig. 9*e* and *f*). The antagonist reverted all these effects (not shown).

Cell adhesion, migration and invasiveness

The effects of the treatments on cell adhesion, migration and invasiveness representing the biologic basis of glioblastoma malignancy, as well as the zymogram for MPP2, are shown in Figure 10. CLA increased cell adhesion on the different supports examined; the PPARγ agonist exerted similar, though weaker, effect. Cell migration and invasiveness were inhibited by both treatments, with CLA again being more effective. The zymogram shows that both CLA and GW347845X treatments decreased the MPP2 levels. PPARγ antagonist completely reverted both CLA and GW347845X effects on all these parameters.

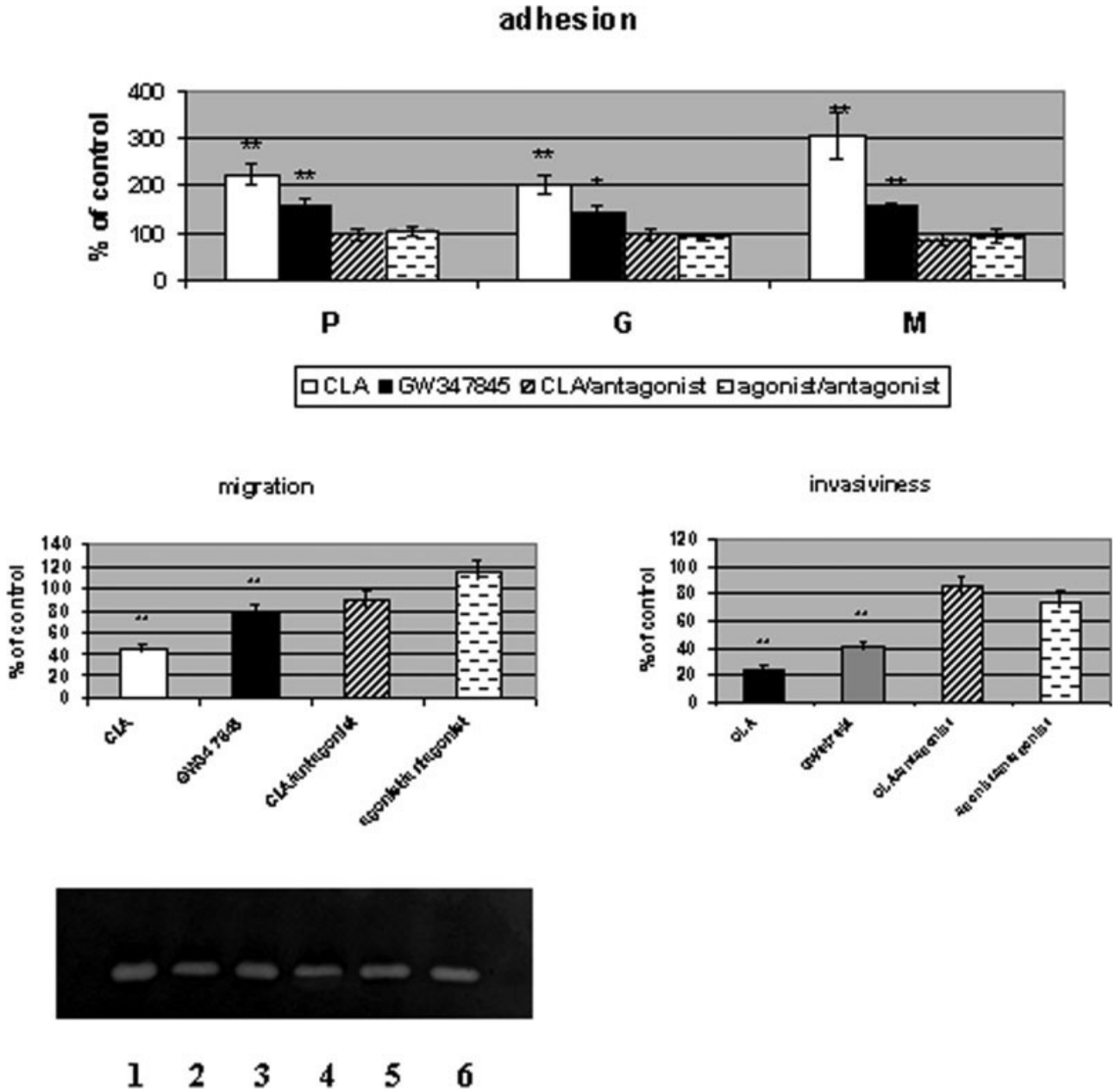

FIGURE 10 – Adhesion, migration and invasiveness assays in control and treated cells. Treatments were for 48 hr. For migration and invasiveness assays, 5 fields/filter were counted. Data are mean ± SD of 3 experiments run in triplicate. Asterisk, $p < 0.01$; double asterisk, $p < 0.001$. One example of zymogram for MPP2 in control and treated cells is also shown. Lane 1, control; lane 2, CLA; lane 3, CLA/antagonist; lane 4, GW347845X; lane 5, GW347845X/antagonist; lane 6, antagonist.

Signal transduction pathway

To investigate which of the possible signal transduction pathways might be involved in some of the observed effects, the levels of the MAPK Erk1,2 (active and inactive forms) were analyzed after a 4-hr treatment (Fig. 11). Both CLA and the γ-agonist decreased the P-ERK1,2 (active form) with respect to the control levels, while the antagonist strongly increased the phosphoprotein level. Samples treated with the associations CLA/antagonist or agonist/antagonist showed similar levels as compared to the controls.

Discussion

While the anticarcinogenic activity of CLA has been extensively studied both *in vivo* and *in vitro* in different tumor cells,[38–42] to our knowledge, this is the first report demonstrating an antitumor activity of CLA on glioblastoma cells. In fact, the only paper dealing with this tumor reported inefficacy of CLA on the human glioblastoma cell line A-172.[43] It is well known that the response of tumor cells to antiproliferative treatments is strongly dependent on their differentiation degree[8] and also influenced by their antioxidant defenses,[44] which are reportedly less efficient in transformed than in normal cells.[45] Indeed, ADF has a higher malignancy grade (grade 4) and lower Se-glutathione peroxidase and GSH levels than A-172 (grade 2).[45,46]

Many of the effects of CLA on both normal and malignant cells have been reported to be mediated by induction and activation of PPARs.[12–14,47] Since in a previous study we demonstrated the presence of PPARs in ADF glioblastoma cells,[8] we

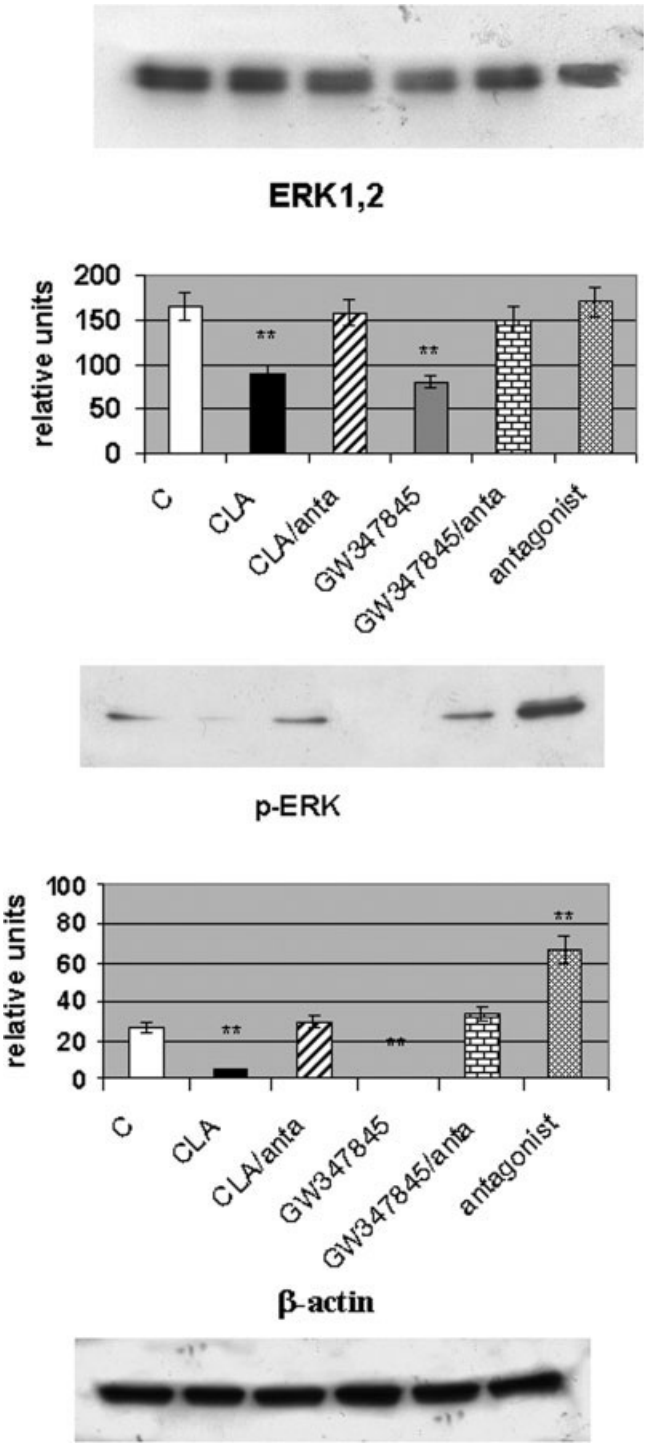

FIGURE 11 – Western blotting and relative densitometric analyses of Erk1,2 (inactive form) and P-Erk1,2 (active form) in control and treated cells. Treatments were for 4 hr. As loading control, β-actin is shown. The densitometric data are mean ± SD of 3 experiments. Asterisk, $p < 0.01$; double asterisk, $p < 0.001$.

hypothesized that even in this cell line the growth-inhibitory effects of CLA might be mediated by PPARγ activation. We particularly focused on PPARγ, as this isotype has long been involved in carcinogenesis.[25,26] To address this issue, the effects of CLA were compared with those of GW347845X, a specific synthetic agonist of PPARγ. The effect of both treatments on PPARγ activation, which was also investigated by a specific ELISA transactivation assay, paralleled a reduction in cell growth and proliferation and an increase of apoptotic rate, thus suggesting that CLA effects are indeed mediated by PPARγ activation. This conclusion is supported by the observation that PPARγ antagonist completely reverted both CLA and GW347845X effects on cell growth and apoptosis. To get a deeper insight into the mechanisms leading to CLA-induced death, we studied the effects of CLA and γ-agonist on caspase-3 and -9 activation. Both treatments activated these 2 caspases, with the γ-agonist more effective on caspase-9. However, the activation of caspases is not exclusively PPARγ-dependent, since the antagonist was unable to revert this effect completely. These observations suggest that CLA and, more surprisingly, even the γ-agonist induce apoptosis also by mechanism(s) other than PPARγ activation. In this respect, it is worth mentioning that recent works point to oxidative stress-mediated effects of specific PPARγ ligands, such as PGJ2 or TZD.[48] A somewhat similar result was obtained when the transactivation of PPARγ by CLA or agonist treatments was assayed. Also in this case, while both treatments transactivated PPARγ, only CLA-mediated effect was completely reverted by the antagonist. This result may be due to the antagonist concentration and/or preincubation time, insufficient to inhibit the rapid effects of the specific agonist. However, higher antagonist concentrations (5–10 μM) were toxic for our cells (not shown).

Since PPARγ ligands are known to induce both expression of PPARγ gene and stabilization of PPARγ protein,[49] we also investigated the patterns of PPARγ mRNA and protein by RT-PCR and Western blotting, respectively. Induction of PPARγ mRNA and protein by both treatments and complete reversion of these effects by the antagonist were observed. Immunofluorescence results confirmed this conclusion and showed that the transcription factor is localized to the nucleus, *i.e.*, the cell compartment where it exerts its functions.

As PPARγ not only plays a crucial role in apoptosis but also in differentiation of a variety of cells, and induction of differentiation has been observed in several malignant cells,[50,51] we investigated whether PPARγ activation would influence differentiation of glioma cells assessed by the glioma differentiation marker N-cadherin.[52] Interestingly, decreased levels of N-cadherin were correlated with dissemination at the time of glioblastoma recurrence in patients.[53] In our experimental conditions, CLA and, to a lesser extent, GW347845X treatments induced some morphologic changes in treated cells such as cellular spreading and elongation of cellular processes as well as increase of cell-cell contacts. The microfilament organization was particularly affected, since actin filaments appeared more organized and oriented. Also, N-cadherin increased and changed its localization from the cytosol to plasma membranes, indicating that both treatments induced a more differentiated phenotype, as already described for PPARγ agonists in other cellular models.[50,51] However, immunoreactivity to GFAP, typical differentiation marker for astrocytes, was never observed in any of our experimental conditions (not shown). Thus, activation of PPARγ may not only lead to the initiation of a distinct cell death program but also induce redifferentiation of neoplastic glioma cells.

It is known that the metastatic features of glioblastoma may be ascribed to cytoskeleton disorganization and altered cell adhesion molecule localization.[54] The involvement of PPARγ on parameters such as cell adhesion, migration and invasion has not yet been studied on glioblastoma. Both ligands, more evidently CLA, increased cell adhesion to different substrates and decreased cellular migration and invasiveness. Since metalloproteinase release is crucial for cellular migration and invasiveness and PPARγ activation has been involved in this process,[55] we assayed MPP2 in our experimental conditions, showing a decrease after CLA or GW347845X treatments. The PPARγ antagonist completely abolished all these effects, indicating that PPARγ activation may be also involved in these functions.

In most epithelial cancers, sustained ERK1,2 activation has been associated with cellular transformation, proliferation and invasion.[56–58] Analysis of various human primary tumors revealed hyperactivation of ERK1,2 in malignant cells as compared with the surrounding normal tissue.[59–61] Our results show that both treatments led to p-ERK downregulation and that this effect was completely reverted by PPARγ antagonist, pointing again toward the involvement of PPARγ activation in decreasing glioblastoma malignancy.

Taken together, our results demonstrate that CLA is, directly or indirectly, a PPARγ activator, thus strongly suggesting this naturally occurring fatty acid, which is known to cross the blood-brain barrier,[62] as brain antitumor drug and possibly a chemopreventive agent. On the other hand, the γ-agonist, once experimented and validated on man, may represent a useful coadjuvant in glioblastoma therapy and in the prevention of recurrences. Future experiments will focus on the specific conditions that guides neoplastic cells toward redifferentiation and on antineoplastic effects of PPARγ agonists in an *in vivo* model of brain tumors. Since the combination of a growth-inhibitory, proapoptotic and cell-differentiating effect on glioma cells would be favorable, PPARγ agonists may offer a new therapeutic strategy for patients affected by malignant glioma.

Acknowledgements

The authors thank Dr. Maria Angela D'Amico and Barbara D'Angelo for their skillful technical assistance, Dr. Sandra Moreno for critical reading of the manuscript and Dr. T. Willsson, GlaxoSmithKline, for the kind gift of GW347845 and GW259662. Supported by Banco San Paolo, Torino (to R.A.C.), Italian PRIN 2003 (068453-003; to A.M.C.) and Neuromed 1% Sanità 2003 (to M.G. Cifone-Cimini).

References

1. Liu G, Bibus DM, Bode AM, Ma WY, Holman RT, Dong Z. Omega 3 but not omega 6 fatty acids inhibit AP-1 activity and cell transformation in JB6 cells. Proc Natl Acad Sci USA 2001;98:7510–5.
2. Rao CV, Simi B, Hirose Y, Upadhyaya P, El-Bayoumy K, Reddy BS. Mechanisms in the chemoprevention of colon cancer: modulation of protein kinase C, tyrosine protein kinase and diacylglycerol kinase activities by 1,4-phenylenebis-(methylene)selenocyanate and impact of low-fat diet. Int J Oncol 2000;16:519–27.
3. Meterissian S, Kontogiannea M, Murty H, Gupta A. Omega-6 fatty acids can inhibit Fas-mediated apoptosis in a human colorectal carcinoma cell line: a potential mechanism for escape from immune surveillance. Int J Surg Invest 2000;2:253–7.
4. Sauer LA, Dauchy RT, Blask DE. Mechanism for the antitumor and anticachetic effects of n-3 fatty acids. Cancer Res 2000;60:5289–95.
5. Vartak S, McCaw R, Davis CS, Robbins ME, Spector AA. Gamma-linolenic acid (GLA) is cytotoxic to 36B10 malignant rat astrocytoma cells but not to normal rat astrocytes. Br J Cancer 1998;7:1612–20.
6. Xi S, Pham H, Ziboh WA. 15-hydroxyeicosatrienoic acid (15-HETrE) suppresses epidermal hyperproliferation via the modulation of nuclear transcription factor (AP-1) and apoptosis. Arch Dermatol Res 2000; 292:397–403.
7. Ziboh VA, Miller CC, Cho Y. Metabolism of polyunsaturated fatty acids by skin epidermal enzymes: generation of antiinflammatory and antiproliferative metabolites. Am J Clin Nutr 2000;71:361S–6S.
8. Maggiora M, Bologna M, Cerù MP, Possati L, Angelucci A, Cimini A, Miglietta A, Bozzo F, Muzio G, Canuto RA. An overview on the effect of linoelic and conjugated linoleic acid on growth of several human tumour cell lines. Int J Cancer 2004;112:909–19.
9. Pariza MW, Park Y, Cook ME. Conjugated linoleic acid and the control of cancer and obesity. Toxicol Sci 1999;52(Suppl):107–10.
10. O'Shea M, Bassaganya-Riera J, Mohede IC. Immunomodulatory properties of conjugated linoleic acid. Am J Clin Nutr 2004;79: 1199S–206S.
11. Field CJ, Schley PD. Evidence for potential mechanisms for the effect of conjugated linoleic acid on tumor metabolism and immune function: lessons from n-3 fatty acids. Am J Clin Nutr 2004;79:1190S–8S.
12. Moya-Camarena S, Vanden Heuvel JP, Blanchard SG, Leesnitzer LA, Belury MA. Conjugated linoleic acid is a potent naturally occurring ligand and activator of PPARα. J Lipid Res 1999;40:1426–32.
13. Moya-Camarena S, Vanden Heuvel JP, Belury MA. Conjugated linoleic acid activates peroxisome proliferator-activated receptor α and β subtypes but does not induce hepatic peroxisome proliferation in Sprague-Dawley rats. Biochim Biophys Acta 1999;1436:331–42.
14. McCarthy MF. Activation of PPARgamma may mediate a portion of the anticancer activity of conjugated linoliec acid. Med Hypotheses 2000;55:187–8.
15. Issemann I, Green S. Activation of a member of the steroid hormone receptor superfamily by peroxisome proliferators. Nature 1990;347: 645–50.
16. Kersten S, Wahli W. Peroxisome proliferator activated receptor agonists. Experientia 2000;89:141–51.
17. Khan SA, Vanden Heuvel JP. Role of nuclear receptors in the regulation of gene expression by dietary fatty acids. J Nutr Biochem 2003; 14:554–67.
18. Gupta RA, Brockman JA, Sarraf P, Willson TM, DuBois RN. Target genes of peroxisome proliferator-activated receptor gamma in colorectal cancer cells. J Biol Chem 2001;276:29681–7.
19. Kliewer SA, Forman BM, Blumberg B, Ong ES, Borgmeyer U, Mangelsdorf DJ, Umesono K, Evans RM. Differential expression and activation of a family of murine peroxisome proliferator-activated receptors. Proc Natl Acad Sci USA 1994;91:7355–9.
20. Escher P, Wahli W. Peroxisome proliferator-activated receptors: insight into multiple cellular functions. Mutat Res 2000;448:121–38.
21. Spiegelman BM. PPAR-gamma: adipogenic regulator and thiazolidinedione receptor. Diabetes 1998;47:507–14.
22. Kliewer SA, Lenhard JM, Willson TM, Patel I, Morris DC, Lehmann JM. A prostaglandin J2 metabolite binds peroxisome proliferator-activated receptor gamma and promotes adipocyte differentiation. Cell 1995;83:813–9.
23. Forman BM, Tontonoz P, Chen J, Brun RP, Spiegelman BM, Evans RM. 15-deoxy-delta-12, 14-prostaglandin J2 is a ligand for the adipocyte determination factor PPAR gamma. Cell 1995;83:803–12.
24. Bar-Tana J. Peroxisome proliferator-activated receptor gamma (PPAR-gamma) activation and its consequences in humans. Toxicol Lett 2001;120:9–19.
25. Theocharis S, Margeli A, Vielh P, Kouraklis G. Peroxisome proliferator-activated receptor-gamma ligands as cell-cycle modulators. Cancer Treat Rev 2004;30:545–54.
26. Michalik L, Desvergne B, Wahli W. Peroxisome-proliferator-activated receptors and cancers: complex stories. Nat Rev Cancer 2004;4:61–70.
27. Leibowitz SB, Kantoff PW. Differentiating agents and the treatment of prostate cancer: vitamin D3 and peroxisome proliferator-activated receptor gamma ligands. Semin Oncol 2003;30:698–708.
28. Kopelovich L, Fay JR, Glazer RI, Crowell JA. Peroxisome proliferator-activated receptor modulators as potential chemopreventive agents. Mol Cancer Ther 2002;1:357–63.
29. Holland EC. Progenitor cells and glioma formation. Curr Opin Neurol 2001;14:683–8.
30. Prins RM, Incardona F, Lau R, Lee P, Claus S, Zhang W, Black KL, Wheeler CJ. Characterization of defective $CD4^{-}CD8^{-}$ T cells in murine tumors generated independent of antigen specificity. Immunology 2004;172:1602–11.
31. Moynihan T, Grossman S. The role of chemiotherapy in the treatment of primary tumors of the central nervous system. Cancer Invest 1994;12:88–97.
32. Cimini A, Cristiano L, Bernardo A, Farioli-Vecchioli S, Stefanini S, Cerù MP. Presence and inducibility of peroxisomes in a human glioblastoma cell line. Biochim Biophys Acta 2000;1474:397–409.
33. Chattopadhyay N, Singh D, Heese O, Godbole MM, Sinohara T, Balck PM, Brown E. Expression of peroxisome proliferator-activated receptors (PPARs) in human astrocytic cells: PPARγ agonists as inducers of apoptosis. J Neurosci 2000;61:67–74.
34. Nwankwo JO, Robbins ME. Peroxisome proliferator-activated receptor-gamma expression in human malignat brain, breast and prostate-derived cells. Prostaglandin Leukot Essent Fatty Acids 2001;64: 241–5.
35. Liu KG, Lambert MH, Ayscue AH, Henke BR, Leesnitzer LM, Oliver WR Jr, Plunket KD, Xu HE, Sternbach DD, Willson TM. Synthesis and biological activity of L-tyrosine-based PPARgamma agonists with reduced molecular weight. Bioorg Med Chem Lett 2001;11: 3111–3.
36. Laemmli EK. Cleavage of structural proteins during the assembly of the head of bacteriophage T4. Nature 1970;227:680–5.
37. Nugent C, Prins JB, Whitehead JP, Savage D, Wentworth JM, Chatterjee VK, O'Rahilly S. Potentiation of glucose uptake in 3T3-L1 adipocytes by PPAR gamma agonists is maintained in cells expressing a PPAR gamma dominant-negative mutant: evidence for selectivity in

the downstream responses to PPAR gamma activation. Mol Endocrinol 2001;15:1729–38.
38. Ip C, Scimeca JA. Conjugated linoleic acid and linoleic acid are distinctive modultors of mammary carcinogenesis. Nutr Cancer 1997;27: 131–5.
39. Kritchevsky D. Antimutagenic and some other effects of conjugated linoleic acid. Br J Nutr 2000;83:459–65.
40. Pariza MW, Park Y, Cook ME. Mechanism of action of conjugated linoleic acid: evidence and speculation. Proc Soc Exp Biol Med 2000;223:8–13.
41. Belury MA. Inhibition of carcinogenesis by conjugated linoleic acid: potential mechanisms of action. J Nutr 2002;132:2995–8.
42. Palombo JD, Granguly A, Bistrian BR, Menard MP. The antiproliferative effects of biologically active isomers of conjugated linoleic acid on human colorectal and prostatic cells. Cancer Lett 2002;177: 163–72.
43. Schonberg SA, Krokan HE. The inhibitory effect of conjugated dienoic derivatives (CLA) of linoleic acid on the growth of human tumor cell lines is in part due to increased lipid peroxidation. Anticancer Res 1995;15:1241–6.
44. Schonberg SA, Rudra PK, Noding R, Skorpen F, Bjerve KS, Krokan HE. Evidence that changes in Se-glutathione peroxidase levels affect the sensitivity of human tuour cell lines to n-3 fatty acids. Carcinogenesis 1997;18:1897–904.
45. Cimini A, Brunori A, Candi E, Catani MV, Cerù MP. Catalase activity in neuroectodermal cell lines and tumors. Clin Chem Enzym Comms 1993;6:63–7.
46. Amicarelli F, Colafarina S, Cattani F, Cimini A, Di Ilio C, Cerù MP, Miranda M. Scavenging systems efficiency is crucial for cell resistance to ROS-mediated methylglyoxal injury. Free Radical Biol Med 2003;35:856–71.
47. Bassaganya-Riera J, Hontecillas R, Beitz DC. Colonic anti-inflammatory mechanisms of conjugated linoleic acid. Clin Nutr 2002;21: 451–9.
48. Winnett G, van Hagen D, Schrey M. Prostaglandin J2 metabolites inhibit aromatase activity by redox-sensitive mechanisms: potential implications for breast cancer therapy. Int J Cancer 2003;103:600–5.
49. Takamura T, Nohara E, Nagai Y, Kobayashi K. Stage-specific effects of a thiazolidinedione on proliferation, differentiation and PPARgamma mRNA expression in 3T3-L1 adipocytes. Eur J Pharmacol 2001;422:23–9.
50. Tontonoz P, Singer S, Forman BM, Sarraf P, Fletcher JA, Fletcher CD, Brun RP, Mueller E, Altiok S, Oppenheim H, Evans RM, Spiegelman BM. Terminal differentiation of human liposarcoma cells induced by ligands for peroxisome proliferator-activated receptor gamma and the retinoid X receptor. Proc Natl Acad Sci USA 1997; 94:237–41.
51. Mueller E, Sarraf P, Tontonoz P, Evans RM, Martin KJ, Zhang M, Fletcher C, Singer S, Spiegelman BM. Terminal differentiation of human breast cancer through PPAR gamma. Mol Cell 1998;1:465–70.
52. Zander T, Kraus JA, Grommes C, Schlegel U, Feinstein D, Klockgether T, Landreth G, Koenigsknecht J, Heneka MT. Induction of apoptosis in human and rat glioma by agonists of the nuclear receptor PPARgamma. J Neurochem 2002;81:1052–60.
53. Asano K, Kubo O, Tajika Y, Takakura K, Suzuki S. Expression of cadherin and CSF dissemination in malignant astrocytic tumors. Neurosurg Rev 2002;23:39–44.
54. Perego C, Vanoni C, Massari S, Raimondi A, Pola S, Cattaneo MG, Francolini M, Vicentini LM, Pietrini G. Invasive behaviour of glioblastoma cell lines is associated with altered organisation of the cadherin-catenin adhesion system. J Cell Sci 2002;115:3331–40.
55. Worley JR, Baugh MD, Hughes DA, Edwards DR, Hogan A, Sampson MJ, Gavrilovic J. Metalloproteinase expression in PMA-stimulated THP-1 cells: effects of peroxisome proliferator-activated receptor-gamma (PPAR gamma) agonists and 9-cis-retinoic acid. J Biol Chem 2003;278:51340–6.
56. Nishida E, Gotoh Y. The MAP kinase cascade is essential for diverse signal transduction pathways. Trends Biochem Sci 1993;18:128–31.
57. Marshall JC. MAP kinase kinase kinase, MAP kinase kinase and MAP kinase. Curr Opin Genet Dev 1994;4:82–9.
58. Krueger JS, Keshamouni VG, Atanaskova N, Reddy KB. Temporal and quantitative regulation of mitogen-activated protein kinase (MAPK) modulates cell motility and invasion. Oncogene 2001;20: 4209–18.
59. Keshamouni VG, Mattingly RR, Reddy KB. Mechanism of 17-beta-estradiol-induced Erk1/2 activation in breast cancer cells: a role for HER2 AND PKC-delta. J Biol Chem 2002;277:22558–65.
60. Sivaraman VS, Wang H, Nouvo GJ, Malbon CC. Hyperexpression of mitogen-activated protein kinase in human breast cancer. J Clin Invest 1997;99:1478–83.
61. Mandell JW, Hussaini IM, Zecevic M, Weber MJ, VandenBerg SR. *In situ* visualization of intratumor growth factor signaling: immunohistochemical localization of activated ERK/MAP kinase in glial neoplasms. Am J Pathol 1998;153:1411–23.
62. Spector R. Fatty acid transport through the blood brain barrier. J Neurochem 1988;50:639–43.